# I. Experimental Facts

## Water-Nonionic Surfactant Systems, and the Effect of Additives

**R. Strey**

Max-Planck-Institut für Biophysikalische Chemie, Postfach 2841, D-37018 Göttingen, Germany

*Key Words: Electron Microscopy / Liquids / Microemulsions / Phase Diagram / Spontaneous Curvature / Water-Nonionic Surfactant*

In this introductory article we approach microemulsions from the binary water-surfactant side. Model systems of the water – nonionic surfactant ($C_iE_j$) type are examined. Many features of microemulsions are observable in these binary systems. As such we discuss the dependence of the cloud points on i and j, the temperature dependence of the viscosity within the micellar phase, and the formation of dilute bilayer phases. The effect of additives is examined, as it permits to gain insight into the structures and interactions. Towards the end of the paper the most important additive for microemulsion formation, the oil, is considered. A special feature of long-chain surfactants is highlighted, namely, non-monotonic critical lines leading to very peculiar two-phase lobes as precursors to the formation of the three-phase bodies.

### 1. Introduction

The phase behavior as well as the microstructure of microemulsions, ternary mixtures of water, oil and surfactant possessing an internal interface, is determined by the interplay of the three binary side systems: Water-surfactant, oil-surfactant and water-oil. The latter system is the most simple one, exhibiting only immiscibility of water and oil. The oil-surfactant system shows a lower miscibility gap with upper critical consolute point, but no mesophases. The most important and by far the one with the richest phase behavior and microstructure is the binary system water-surfactant. For a recent review of water-surfactant systems the reader is referred to R.G. Laughlin's monograph [1]. There a large variety of different surfactants are examined.

### 2. Binary Water-Nonionic Surfactant Systems

We confine ourselves here to model systems of the type $H_2O - C_iE_j$ (n-alkyl polyoxyethylene ether). At first we shall consider, which phases are observed, and how they vary with the lengths of the hydrophobic tail i and the hydrophilic head j.

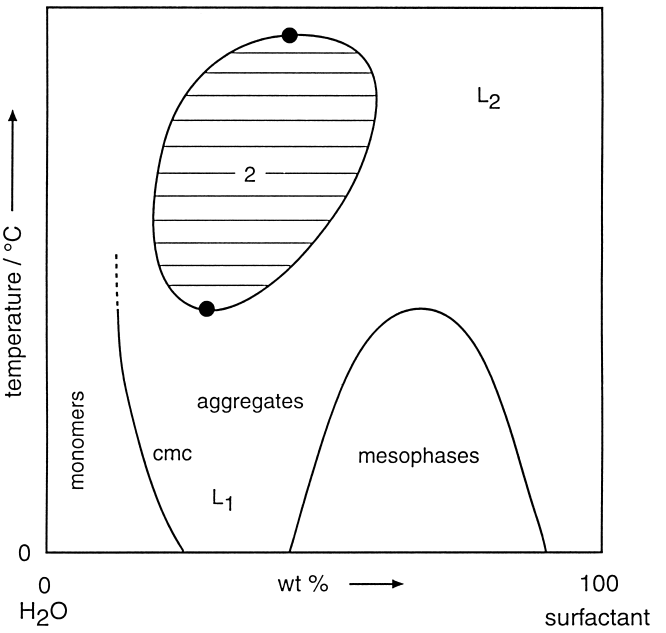


Fig. 1
Schematic phase diagram of a binary water – nonionic surfactant system

#### Model Systems

Let us start with a schematic picture (Fig. 1), which we subsequently will elucidate with selected experimental material.

At very low surfactant concentrations the surfactant dissolves in the form of monomers. Increasing the surfactant concentration the critical micelle concentration is passed (see Fig. 1). From now on further added surfactant will form micelles, aggregates of about 100 surfactant molecules, until the concentration becomes sufficiently high that lyotropic mesophases form. Historically, the isotropic micellar phase has been denoted $L_1$. Surfactant-rich solutions are usually referred to as $L_2$.

For the nonionic surfactants $C_iE_j$ we are concerned with here, increasing the temperature leads to dehydration of the surfactant and hence to phase separation into a surfactant-rich and a surfactant-lean phase at the so-called cloud point curve, an upper miscibility gap with lower consolute (critical point). In some cases one can even see the upper gap close [2]. Then a closed loop is formed. The lower critical point is, in general, located at low surfactant concentration. Values of the order of 1 wt.% are not uncommon [3]. The upper critical point is generally located above the boiling point [2, 4]. Open questions are the detailed microstructure inside the $L_1$ region as the surfactant concentration increases towards $L_2$. In particular, the surfactant-rich phase of the loop is still poorly understood. Also unknown is the fate of cmc-curve as the temperature increases. Does it pass the loop or intersect it at some point?

  *0005-9021/96/0303-0182 $ 15.00+.25/0*

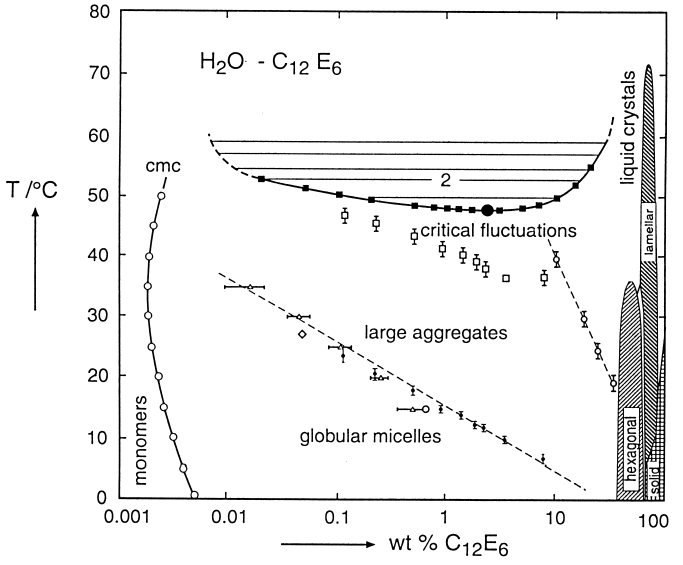


Fig. 2
Phase diagram for the water-$C_{12}E_6$ system (after Pakusch and Strey [5])

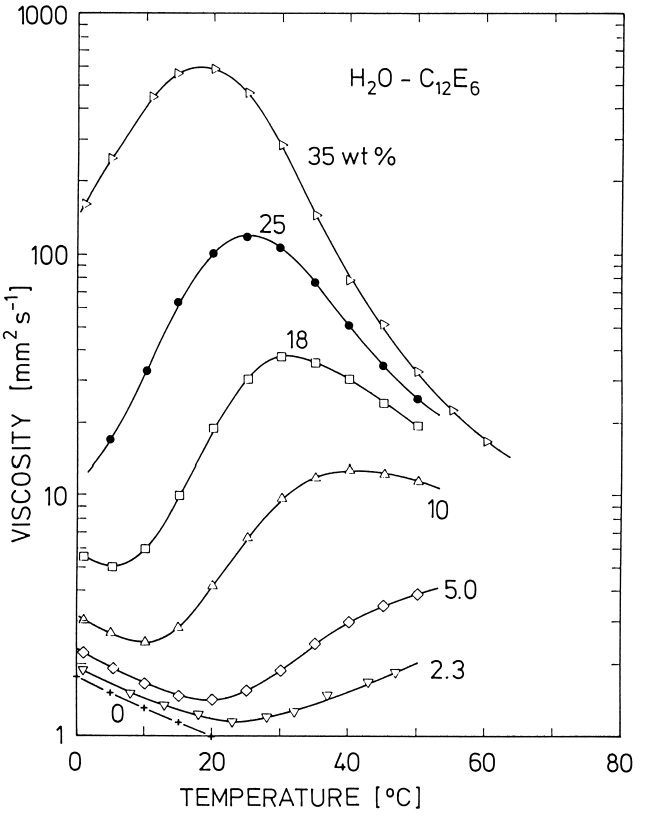


Fig. 3
Dynamic shear-viscosity for water-$C_{12}E_6$

An actual phase diagram for the water-$C_{12}E_6$ system determined by Pakusch and Strey [5] is shown in Fig. 2.

A logarithmic concentration axis is chosen in order to resolve all interesting points. Indicated is the upper loop with the coexisting 2 phases with the lower critical point near $T_\beta = 50\,°C$. Also the cmc-curve located around concentrations of 0.002 wt.% surfactant is shown. It is experimentally difficult to decide how the loop continues towards low concentrations. Using dynamic light scattering in conjunction with the T-jump technique, one could determine the range where the dynamics of the system were governed by critical concentration fluctuations [6] in contrast to those regions were large micellar aggregates or globular micelles are present [7, 8]. The discrimination of globular, near-spherical micelles from large aggregates is obtained from the increasingly larger amplitude and smaller relaxation times of the T-jump signal with increasing temperature.

## Shear-Viscosity

The dividing line between globular and larger aggregates in Fig. 2 exhibits itself in the dynamic viscosity measured as function of temperature (Fig. 3). Interestingly, with increasing temperature the viscosity *increases*, an indication for the structural change at the dividing line at low temperatures.

As temperature further increases the viscosity curves run through maxima indicating yet another structural change. The line connecting the maxima is also indicated in Fig. 2. With increasing concentration it declines to the shoulder of the hexagonal phase $H_1$.

At higher concentrations one can see in Fig. 2 the lamellar phase $L_\alpha$ exist. Sandwiched in between is the viscous isotropic phase $V_1$ [9]. By analogy with related $C_{12}E_7$ and $C_{12}E_8$ systems, a cubic phase $I_1$ (an ordered phase of globular micelles) might be expected below O °C in the undercooled state [9]. It is, however, not shown in Fig. 2. This is remarkable in so far as the demarcation line between globular and larger aggregates intersects below O °C with $H_1$.

For this particular system the lamellar mesophase is well-separated from the upper loop. This is not the case, if the relative hydrophilicity of the surfactant is decreased [10, 11]. We will return to this point further below.

## Cloud Point Curves

Decreasing the number of ethylene oxide units j of the surfactant the miscibility gap is lowered on the temperature scale (see Fig. 4).

Schubert et al. [3] have measured the $T_\beta$'s for a whole range of purified water-$C_iE_j$ surfactants. For a wide range of chain length i the same observation is made: For a given i, the lower the ethylene oxide number j, the lower the critical temperature $T_\beta$. Also the critical concentration $\gamma_c$ ($\gamma$ is the surfactant concentration in wt.%) is shifted to lower concentrations.

For a given j, the miscibility gaps show systematic variations (Fig. 5) with the carbon number i of the tail.

With decreasing i the gaps are shifted to higher temperatures. At the same time the gaps become more narrow concentration-wise. The width of the miscibility gaps decreases by one order of magnitude per 2 carbon atoms. At the same time $\gamma_c$ increases. It is interesting to note that in each case the cmc-curve closely marks the lower end of the gaps.

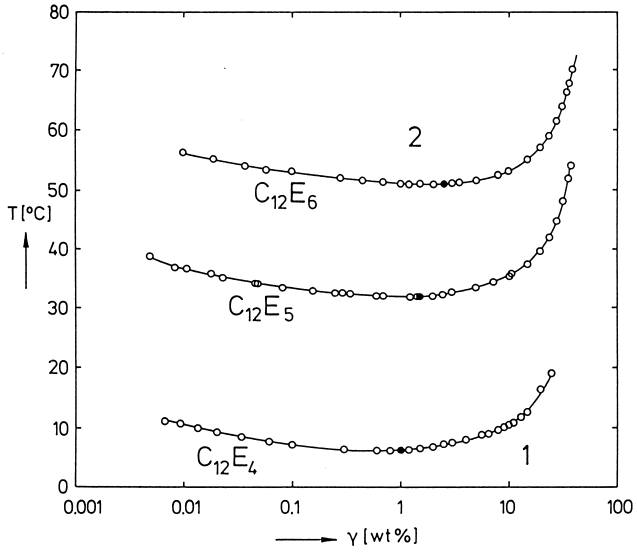


Fig. 4
Miscibility gaps as function of j

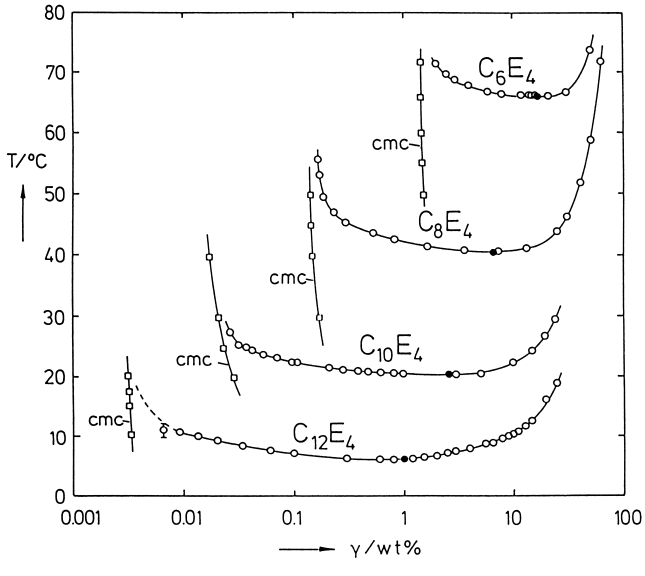


Fig. 5
Miscibility gaps as function of i

## Dilute Lamellar and $L_3$ Phases

From previous work of Harusawa et al. [12] in 1974 and Mitchell et al. [9] in 1983 it was known that the lamellar phase for $C_{12}E_5$ intersects with the upper miscibility gap. However, the exact extent of the lamellar phase toward low surfactant concentrations remained unknown. Strey et al. [11] in 1990 clarified this point and showed that the lamellar phase (Fig. 6) may be extremely diluted down to 1 wt% of surfactant.

At such low surfactant concentrations the repeat distance of the lamellae becomes of the order of the wavelength of visible light [11]. Hence, the surfactant solutions scattered light which gives the solutions a brilliant appearance. Such observations have earlier been made with related 3 and 4

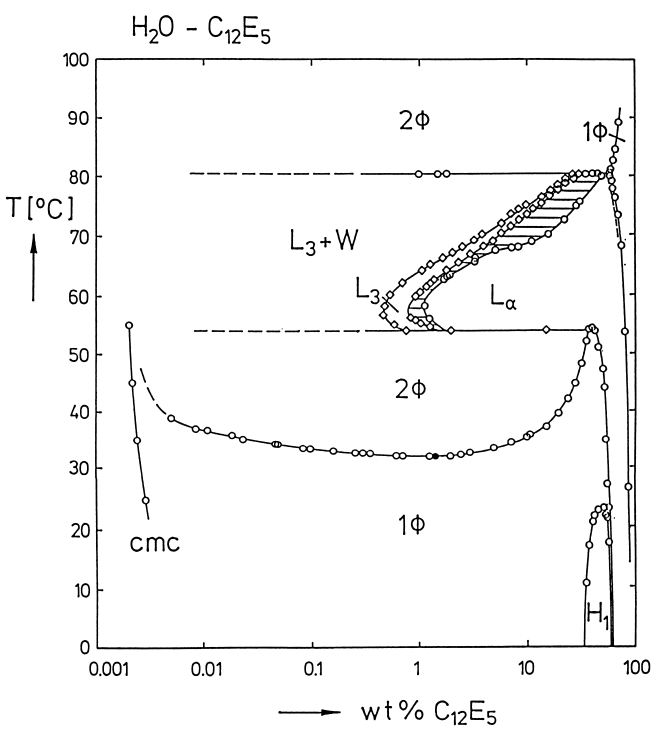


Fig. 6
Phase diagram for water-$C_{12}E_5$

component systems, including ionic surfactants, brine and cosurfactants [13, 14].

The phase diagram for water-$C_{12}E_5$ in Fig. 6 shows the relative location of the upper loop and the intersecting dilute lamellar phase. One notes in agreement with the previous workers at higher temperatures the transition to an $L_3$ phase [9, 12]. In an $L_3$ phase the bilayers of the lamellar phase have been torqued into a three-dimensional multiply connected network of bilayers [15]. Towards lower concentrations the $L_3$ phase coexists with an almost pure water phase in which recently large structures have been detected [16]. It is difficult to decide whether these were only the remnant of an incomplete phase separation process, or real structures of an unknown phase located at surfactant concentrations below 0.1 wt.%. A detailed discussion has to be postponed to a later date.

Also indicated in Fig. 6 is the cmc, which is apparently only little influenced by the change of ethylene oxide units, relative to the water-$C_{12}E_6$ system in Fig. 2.

## The $L_\alpha^+$ Region

In Fig. 7 the (still incomplete) phase diagram for water-$C_{12}E_4$ demonstrates, how large the extent of the lamellar phase may become temperaturewise.

As for $C_{12}E_5$ the lamellar phase extends towards low surfactant concentration with a maximal extension around 49 °C. Again the $L_3$ phase is located temperaturewise above it. As seen already in Fig. 4, the loop is located at low temperatures. Its extent, as far as it can be experimentally traced, is bounded again by the cmc. As temperature is increased above 22.5 °C a transition into the lamellar phase occurs.

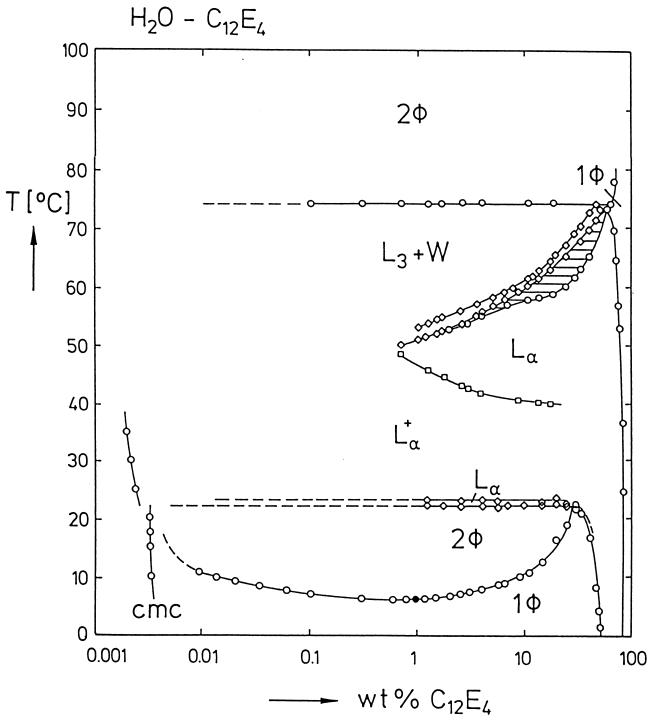


Fig. 7
Phase diagram for water-$C_{12}E_4$ (still incomplete)

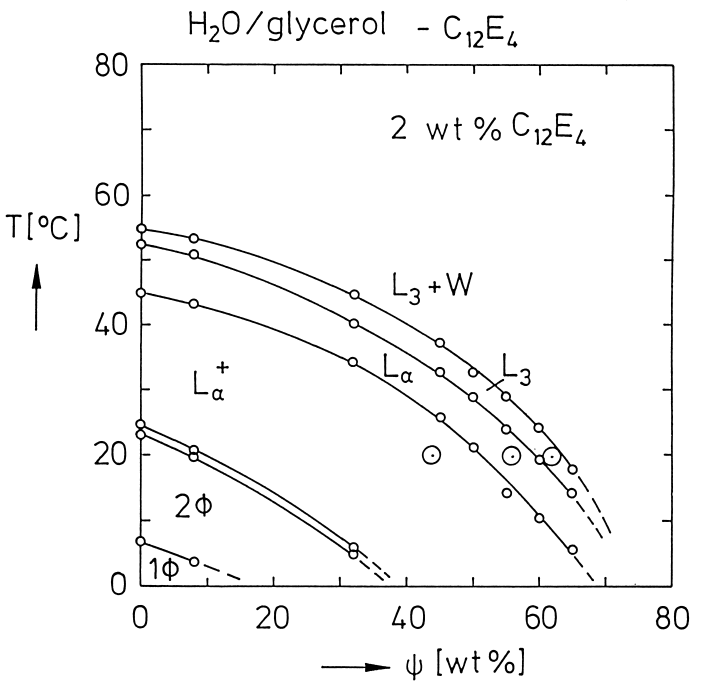


Fig. 8
Effect of glycerol on the binary water-$C_{12}E_4$ system. $\psi$ are wt.% of glycerol in the water/glycerol mixture

It is interesting to note that the cmc-curve determined by surface tension measurements [17] shows a break at the transition from the coexistence of the isotropic 2 phase region of the loop to the lamellar phase $L_\alpha$. The anisotropic, lamellar nature has been verified by scattering techniques and polarization microscopy. Only one degree higher at 23.5 °C stirred samples transform into a strongly streaming-birefringent and strongly scattering state, which we termed $L_\alpha^+$ [20]. The structure of the $L_\alpha^+$ region is not yet very well-known [18]. It appears as if the lamellar structure is simply destroyed by shear and then cannot reform because of an energy barrier. Here freeze-fracture-electron microscopy (FFEM), which has been applied to bilayer phases before [19], might be a useful technique.

## 3. Effect of Additives

For electron microscopic preparation of the water-nonionic surfactant systems there is quite generally the problem that samples from elevated temperature have to pass through the 2 phase region and then through the micellar region (see e.g. Fig. 6 or 7). For this reason many previous attempts of cryo-fixation of the structures were unsuccessful.

### Effect of Glycerol

There is, however, a possibility to lower the phase under question to room temperature by mixing water and glycerol which form a pseudo-component. Such combinations may be used to affect the phase behavior by the competition of glycerol and surfactant head groups for the water. Fig. 8 shows the lowering of the binary water-$C_{12}E_4$ system by gradually replacing water with glycerol. $\psi$ stands for the weight ratio of glycerol in water plus glycerol.

For $\psi = 50$, 57.5 and 60 wt.% indicated by the circles in Fig. 8 we were able to obtain the $L_\alpha^+$, the dilute lamellar and the $L_3$ phase. In Fig. 9 we show pictures by FFEM of $L_\alpha$, $L_\alpha^+$ and $L_3$ for 6 wt.% of surfactant.

For the $L_\alpha^+$ region both single- and multi-shelled, and short tubular vesicles were seen. At much higher concentrations pictures (not shown here) a structure resembling the $L_3$ structure with multilayers in place of the single bilayers was found. The reason for a successful cryofixation may be two-fold. Firstly, the glycerol content increases the viscosity by an order of magnitude. Secondly, cooling toward 0 °C one always stays within the bilayer phases (cf. Fig. 8).

### Sodium Chloride, NaCl

A similar, gradual lowering of the phase transitions on the temperature scale can be generated by adding a lyotropic salt, like NaCl (see Fig. 10, top) [20].

The gradual evolution of $L_\alpha^+$ from the lamellar phase is demonstrated. Here the phase boundaries vary nearly linearly with the additive.

### Less-Hydrophilic Surfactant

The nature of the $L_\alpha^+$ region is one of bilayers, organized differently than in the $L_\alpha$. The continuous evolution or appearance of $L_\alpha^+$ within the region of the dilute lamellar phase has been demonstrated by Jonströmer and Strey [20] in 1992. Fig. 10, center, shows the gradual nature of the

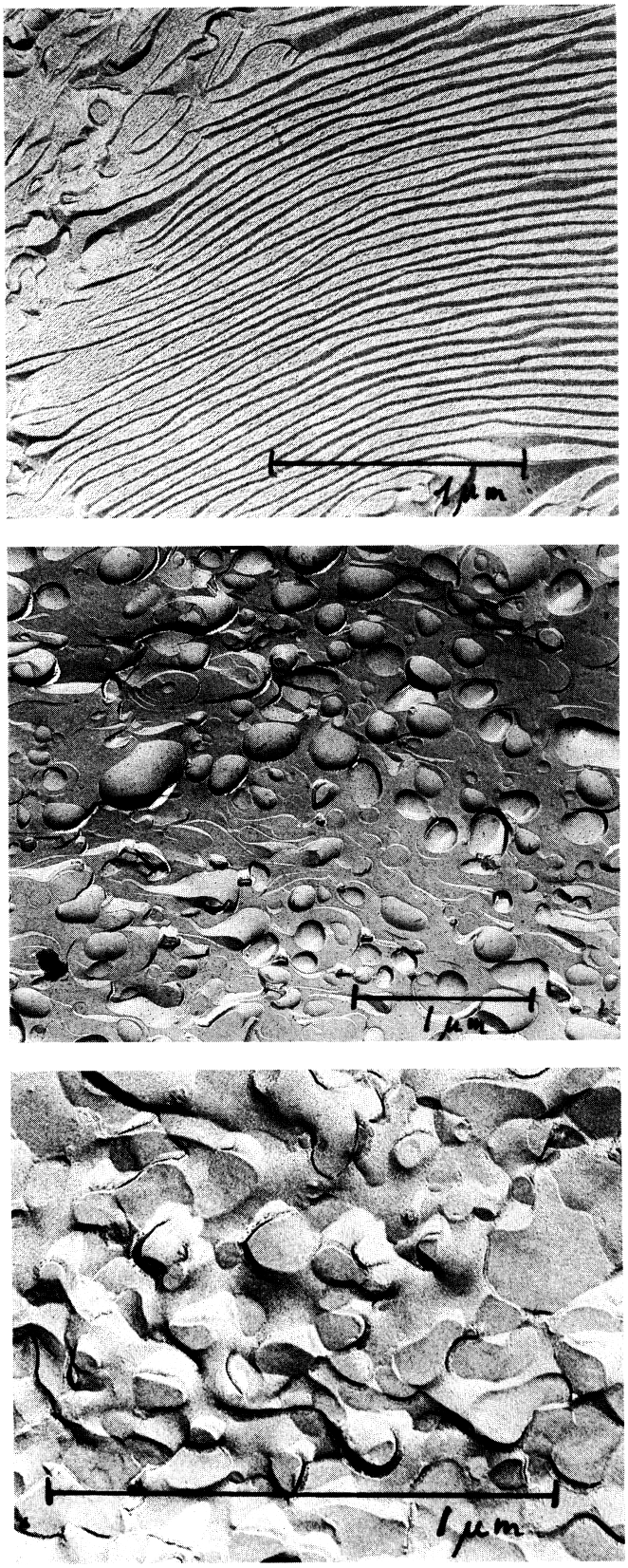


Fig. 9
Dilute bilayer phases: lamellar (top), $L_\alpha^+$ (center) and $L_3$ (bottom)

transition. It is noteworthy that $L_\alpha^+$ is fully imbedded in the lamellar phase and occurs as function of decreasing hydrophilicity of the surfactant. The borderline between $L_\alpha^+$ and $L_\alpha$ is not as sharply defined as the other phase transition temperatures. It depends to some degree on the stirring speed and thermal history. One should, therefore, be careful not to refer to $L_\alpha^+$ as a separate phase than $L_\alpha$. For measuring the phase diagrams in Fig. 10, center, two solutions, one containing water-$C_{12}E_5$ and the other one water-$C_{12}E_3$, were mixed together in various proportions. At a certain ratio in the intermediate range effectively homogeneous $C_{12}E_4$, indicated by the full diamonds, is mimicked by the mixture $C_{12}E_5/C_{12}E_3$. Also seen is the gradual trend of the cloud point curve and the other phases, in particular, the $L_3$ phase. A sample for pure water-$C_{12}E_3$ showed clearly the vesicular nature of the dilute $L_\alpha^+$ phase.

### Alcohol

In Fig. 10, bottom, the analogous trends are generated by the addition of a so-called cosurfactant, here n-hexanol ($C_6E_0$) [20]. The addition of the cosurfactant has again the advantageous feature that one may lower the $L_3$ phase and other dilute phase to room temperature from where FFEM preparation is easy. For this system, we were able to confirm previous observations [19] that the transition between $L_\alpha$ and $L_3$ might occur through the formation of so-called passages (Fig. 11), tubular connections from one bilayer to the next.

In Fig. 11 passages both up and down to the adjacent layers are visible. Interestingly, the addition of a short-chain amphiphile as an alcohol does not destroy the lamellae [20]. On the contrary mixing n-octanol to water-$C_8E_5$, a system not showing any of the dilute phases, the dilute lamellar and $L_3$ phases may be generated [28].

### Shorter-Chain Homologues

Adding instead of an alcohol a shorter chain surfactant e.g. $C_8E_3$ leads after replacing 30% of the $C_{12}E_5$ by $C_8E_3$ molecules to a complete destruction of the bilayer phase. Apparently, a mixed surfactant of effectively shorter chain is formed. Shorter chain surfactants are known not to form dilute bilayer phases [1, 9].

### Oils

Adding oils, e.g. alkanes, to the binary system water-$C_iE_j$ one enters the domain of microemulsions. For review we recommend the feature articles [21 – 23].

As for a number of other additives, the effect of adding oil to the binary system $H_2O - C_iE_j$ is to lower the cloud point. This can nicely be demonstrated by measuring the trajectory of the critical line $cp_\beta$. The critical line $cp_\beta$ starts in the binary system at $T_\beta$ (see Fig. 5, $T_\beta = 20.5\,°C$ for $C_{10}E_4$, [3]) and descends into the phase prism, but then ascends again, until it ends at a critical endpoint, where the three-phase triangle opens up [21]. (A measurement is

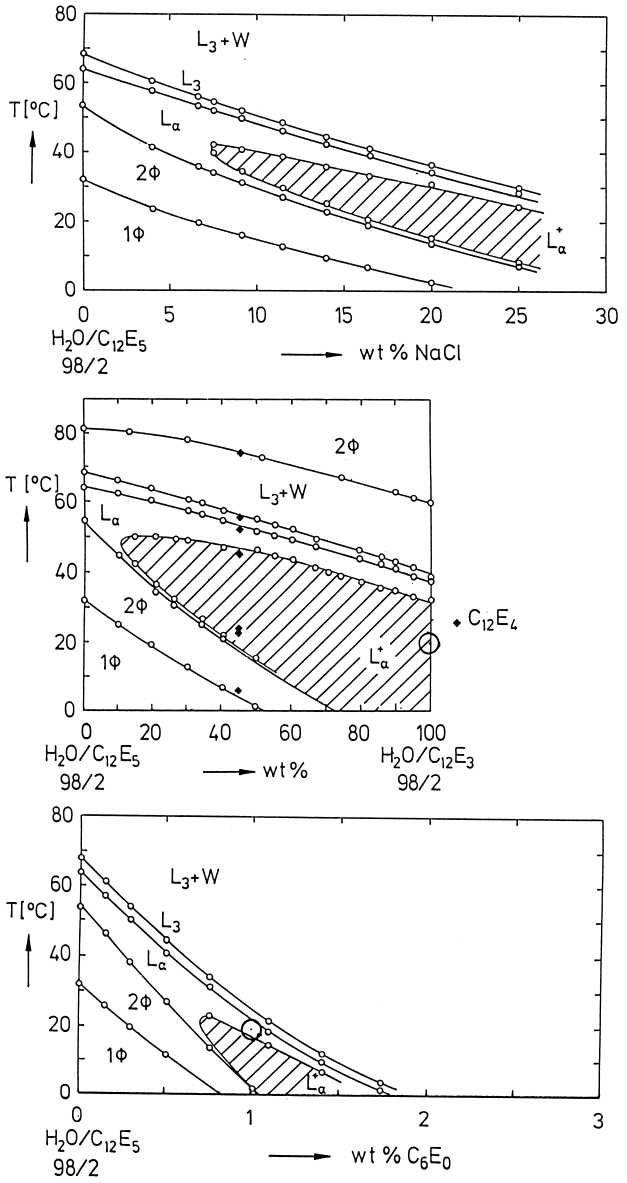


Fig. 10
Effect of additives on the binary system water-$C_{12}E_5$: NaCl, $C_{12}E_3$, n-hexanol ($C_6E_0$) (after Jonströmer and Strey [20])

shown below in Fig. 12). Thus there is an important difference to the other additives mentioned. The three-phase triangle appears when the critical point touches the solubilization (emulsification failure) curve. Interestingly, depending on the chain length of the surfactant there are differences of exact shape of the critical line [22, 23]. While for the short-chain homologues, like $C_4E_1$, the critical line descends monotonically, the line bulges out to become non-monotonic for $C_8E_4$ and the higher homologues [23]. It should be noted that adding oil to the binary water-surfactant system of critical composition permits tracing the critical line to a very good approximation because the cloud point curves (see Figs. 4 and 5) are rather flat.

The non-monotonic behavior of the critical lines for longer chain surfactants has first been reported by Shinoda and

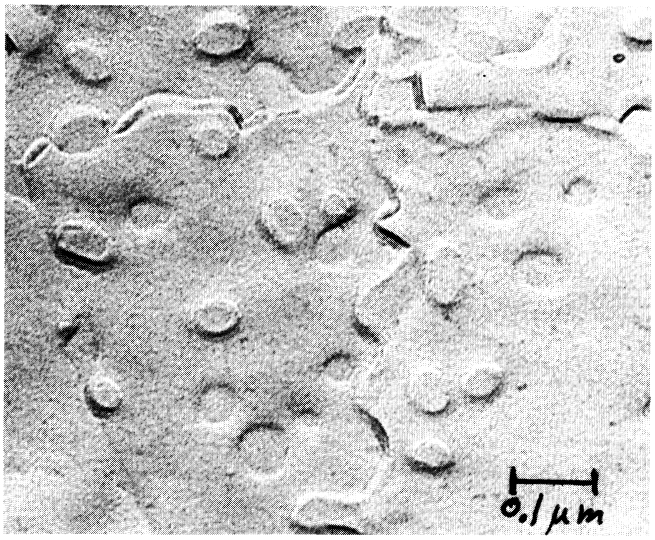


Fig. 11
Formation of so-called passages in the water-$C_{12}E_5 - C_6E_0$ system

coworkers in 1967 [24]. From their work it is also evident that the same phenomenon also occurs on the oil-rich side [25]. That is, starting with surfactant in an oil solution, one observes a non-monotonic critical line and a descending solubilization (emulsification failure) curve. It is of paramount importance to note that on the oil-rich side the phase behavior has the reverse temperature dependence.

A simple system for which both the water and the oil side show non-monotonic critical lines is the water-n-octane-$C_{10}E_4$ system [22]. In Fig. 12 (top, left, full symbols) the temperatures of the critical points are plotted vs. the n-octane ($B_8$) content.

From several such plots one may construct isothermal diagrams. Such an isothermal diagram is shown on Fig. 12 (bottom, left). It reveals that the miscibility gaps take the shape of 2 phase lobes with the tie-lines declining towards the cmc in the respective corner. In the bottom part of Fig. 12 the lobes on the water side (left, $T < T_l$) are compared to those on the oil side (right, $T > T_u$). A striking symmetry is observed. In the top part of Fig. 12 the non-monotonic critical lines (full points) are shown. They end where the critical points touch the solubilization boundary (open symbols) to form the three-phase body existing between $T_l = 21.5\,°C$ and $T_u = 27.9\,°C$. The declination of the tielines towards the cmc is particularly clearly seen on the oil-rich side, where the $cmc_b$ amounts to a few wt.% in oil.

These observations have been summarized in a schematic diagram (Fig. 18 of Ref. [23]). However, Fig. 12 top in conjunction with Fig. 12 bottom suffices to discuss the evolution with *increasing* temperature: As one starts at low temperatures, the solubilization boundary, the binodal, is a nearly straight line intersecting with the water corner, just above the $cmc_a$ (Fig. 12, bottom left). As temperature increases the straight line binodal decreases in slope. At the same time the phase separation tendency, originating from the upper loop of the binary system water-surfactant,

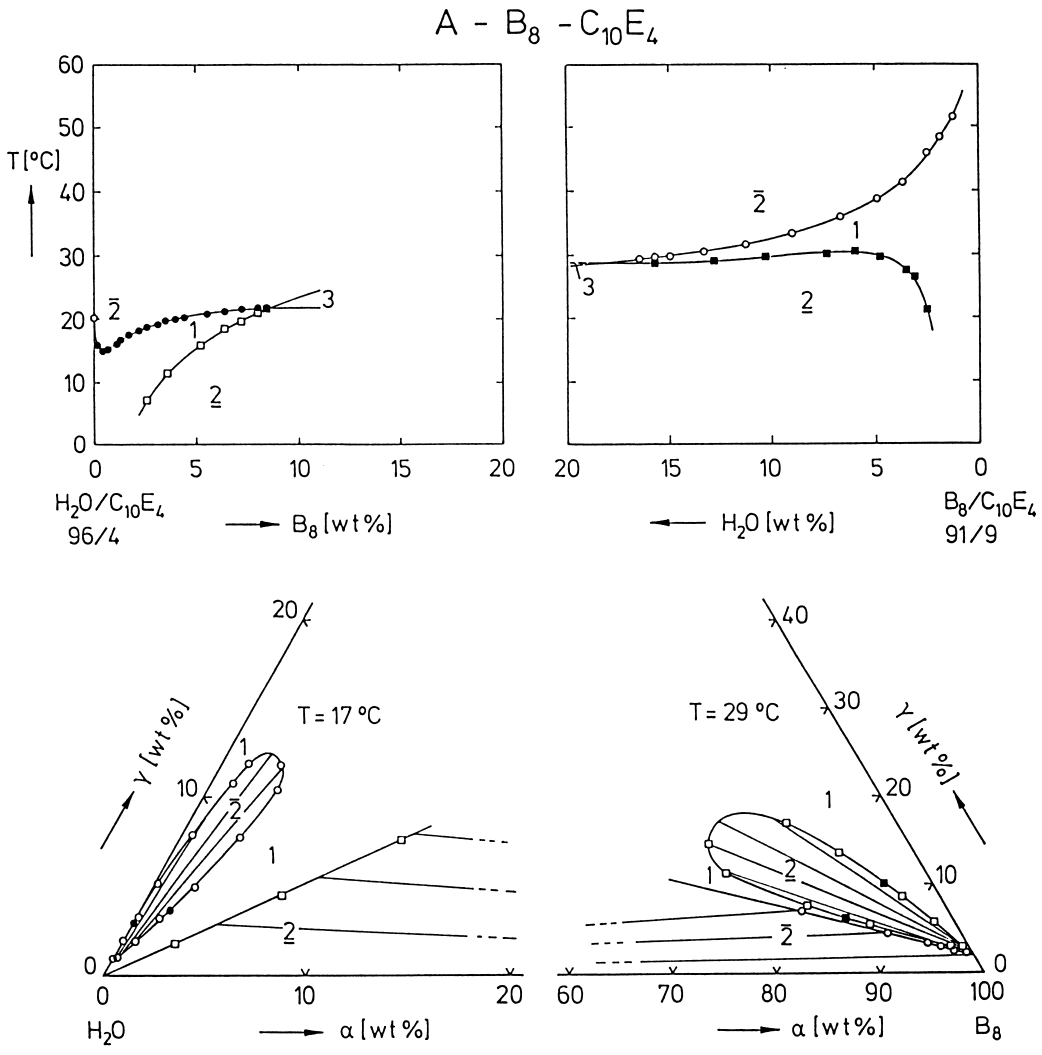


Fig. 12
Effect of n-octane (B8) on the binary system water-$C_{10}E_4$ (top, left). Note the shape and symmetry of the two-phase lobes (bottom). Effect of water on the binary n-octane-$C_{10}E_4$ system (top, right)

becomes stronger until the critical line appears at a bicritical point inside the one phase region. From there it expands into the two-phase lobe exhibiting two critical points. One of them faces the binary system, the other one faces the straight line binodal. The tie-lines in the two-phase lobe decline toward the water corner. The expansion of the two-phase lobe is faster than the change in slope of the binodal. Therefore, further increasing temperature leads to a collision of the inner critical point with the straight line binodal at $T_l$, and the three-phase body appears (Fig. 12, top, left). Thus, the formation of the three-phase body (and all the relevant and important properties associated with it) is driven by a similar force that dictates the behavior in the binary water-surfactant system.

On the oil-rich side the analogous scenario happens with decreasing temperature. Compare Fig. 12, left vs. Fig. 12, right. For high temperatures, the isothermal straight line binodal intersects with the binary oil-surfactant side above the $cmc^b$ in oil. With decreasing temperature the slope of the binodal decreases. As the phase-separation tendency of oil and surfactant becomes strong enough the lobe appears as a bicritical point and expands (Fig. 12, bottom right). The tie-lines in the lobe are declining toward the oil corner. Decreasing temperature further, the inner critical point touches the binodal at $T_u$, and the three-phase triangle opens up on the oil-rich side.

## 4. Conclusion

One can 7 infer that a similar mechanism, which is responsible for the structural changes in the binary water-surfactant system leading to phase separation at the cloud point, is also responsible for the formation of the three-phase triangle on the water-side. The remarkable symmetry suggests that the same mechanism is responsible for the happening on the oil side as well. In this volume Menes et al. [26, 27] present a model including interactions of non-spherical globules. It is shown to predict qualitatively correctly the occurrence of the lobes and the competition with the emulsification boundary. In that paper the microstruc-

ture and phase behavior is assumed to be driven by the temperature variation of the spontaneous curvature. The mean curvature of the interfacial film on the other hand changes monotonically with increasing temperature, as has recently been quantified using electron microscopy and neutron scattering [29].

Therefore one may conclude that the experimentally observed trends in the phase diagrams and structures are the consequence of the variation of the spontaneous curvature with temperature and concentration of the additive.

The present work was performed in the department of Prof. M. Kahlweit to whom we are indebted for continuous exchange of ideas and support.

## References

[1] R.G. Laughlin, "Aqueous Phase Behavior of Surfactants", Academic Press, New York 1994.
[2] J.C. Lang and R.D. Morgan, J. Chem. Phys. *73*, 5849 (1980).
[3] K.-V. Schubert, R. Strey, and M. Kahlweit, J. Colloid Interface Sci. *141*, 21 (1991); Prog. Colloid Polym. Sci. *84*, 103 (1991).
[4] P. Firman, D. Haase, J. Jen, M. Kahlweit, and R. Strey, Langmuir *1*, 718 (1985).
[5] R. Strey and A. Pakusch, "Critical Fluctuations", Proceedings of the 5th International Symposium on "Surfactants in Solution", Bordeaux 1983, ed. by K.L. Mittal and P. Bothorel, Plenum, New York, 465 (1986).
[6] B. Chu, Ber. Bunsenges. Phys. Chem. *76*, 202 (1972).
[7] E.J. Staples and G.T.J. Tiddy, J. Chem. Faraday Trans. I. *74*, 2530 (1978).
[8] R. Triolo, J.L. Magid, J.S. Johnson Jr, and H.R. Child, J. Phys. Chem. *86*, 3689 (1982).
[6] B. Chu, Ber. Bunsenges. Phys. Chem. *76*, 202 (1972).
[7] E.J. Staples and G.T.J. Tiddy, J. Chem. Faraday Trans. I. *74*, 2530 (1978).
[8] R. Triolo, J.L. Magid, J.S. Johnson Jr, and H.R. Child, J. Phys. Chem. *86*, 3689 (1982).
[9] D.J. Mitchell, G.J.T. Tiddy, L. Waring, T. Bostock, and M.P. McDonald, J. Chem. Soc. Faraday Trans. I, *79*, 975 (1983).
[10] M. Kahlweit, R. Strey, and D. Haase, J. Phys. Chem. *89*, 163 (1985).
[11] R. Strey, R. Schomäcker, D. Roux, F. Nallet, and U. Olsson, J. Chem. Soc. Faraday Trans. *86*, 2253 (1990).
[12] F. Harusawa, S. Nakamura, and T. Mitsui, Colloid Polym. Sci. *252*, 613 (1974).
[13] C. Thunig, H. Hoffmann, and G. Platz, Prog. Colloid Polym. Sci. *79*, 297 (1989).
[14] G. Porte, J. Marignan, P. Bassereau, and R. May, J. Phys. (France) *49*, 511 (1988).
[15] G. Porte, J. Phys. Condens. Matter *4*, 8649 (1992).
[16] T. Sottmann and R. Strey, unpublished results.
[17] D. Haase, unpublished results.
[18] U. Olsson and R. Strey, in preparation.
[19] R. Strey, W. Jahn, G. Porte, and P. Bassereau, Langmuir *6*, 1635 (1990).
[20] M. Jonströmer and R. Strey, J. Phys. Chem. *96*, 5993 (1992).
[21] M. Kahlweit and R. Strey, Angew. Chem. Int. Ed. *24*, 654 (1985).
[22] M. Kahlweit, R. Strey, and G. Busse, J. Phys. Chem. *94*, 3881 (1990).
[23] M. Kahlweit, R. Strey, and G. Busse, Phys. Rev. E. *47*, 4197 (1993).
[24] H. Saito and K. Shinoda, J. Colloid Interface Sci. *24*, 10 (1967).
[25] K. Shinoda and T. Ogawa, J. Colloid Interface Sci. *24*, 56 (1967).
[26] R. Menes et al., this volume.
[27] R. Menes, S.A. Safran, and R. Strey, Phys. Rev. Lett. *74*, 3399 (1995).
[28] M.H.G.M. Penders and R. Strey, J. Phys. Chem. *99*, 6091 (1995).
[29] R. Strey, Colloid Polymer Sci. *272*, 1005 (1994).

Presented at the Discussion Meeting of the Deutsche Bunsen-Gesellschaft für Physikalische Chemie "Microemulsions – Experiment and Theory" in Göttingen, September 4th to September 6th, 1995

E 9082